Clay Research, Vol. 42, pp. 26-35 (2023 & 2024)

Identification and characterization of mica minerals in mine spoils and their potential in plant nutrition

NAVYA M. [1, 2] *, SANDEEP S. [2] AND ANIL KUMAR [3]

[1] *Cochin University of Science and Technology, Kochi-682022, Kerala, India*
[2] *KSCSTE- Kerala Forest Research Institute, Peechi-680653, Thrissur, Kerala, India*
[3] *ICAR-National Bureau of Soil Survey and Land Use Planning, Hebbal, Bangalore, 560024, India*

Abstract: *Mica deposits are rich in India, with nearly two thirds discarded as waste during the cleaning and processing stages. In this study waste mica from mica mines in Andhra Pradesh was collected and characterized for its structural, chemical and morphological properties. The elemental composition analysis confirmed the presence of 49.23% SiO_2, 18.26% Al_2O_3, 15.45% MgO, 11.28% Fe_2O_3, and 3.81% K_2O, with the high iron content confirming the waste mica as biotite. The Mg/Fe, Fe/(Fe+Mg) ratio and XRD results further confirms this identification. FTIR, and SEM analyses highlighted the characteristic peaks and morphology of biotite in these mine spoils. Plant growth experiments demonstrated the waste mica/boitie's suitability as a nutrient source, with treated plants exhibiting superior growth compared to control and alternative treatments. This study establishes waste mica/biotite as a promising source for enhancing plant nutrient availability. Field experiments are essential to optimize the combination of waste mica and nutrients, presenting a potentially cost-effective approach for potassium management in hitherto deficient soils.*

Keywords: Bioavailability; Biotite; FTIR; SEM; Waste mica; XRD

Mica deposits are rich in India, with approximately two-thirds of them being discarded as waste during the cleaning and processing stages and having no practical use. Micas refer to a group of phyllosilicates that have interlayer cations firmly linked to one another to counteract the high layer charge. Ideally mica is a complex hydroaluminum silicate with a 2:1 structure consisting of one octahedral gibbsite- or brucite-like sheet sandwiched between two tetrahedral sheets (Fanning and Keramidas, 1977). Mica, the mineral has a plate-like structure with distinct physical characteristics such as colour, density, particle size, shape, layered structure, and reflection index, that make them an ideal mineral for several industrial uses (Perez-Rodriguez *et al.,* 2006; Andric *et al.,* 2014). Three major divisions have been identified within the mica silicates, i.e., the true micas, the brittle micas and the interlayer-deficient micas. This division is further subdivided into dioctahedral (e.g. muscovite, boromuscovite, etc) and trioctahedral groups (e.g. biotite and phlogopite). Of the 37 varieties of mica, the most common are biotite (magnesium–iron), muscovite (potassium–aluminium), phlogopite (potassium–magnesium),

ORCID ID
*** Email ID of Corresponding Author** (Navya M): navyamurali23@gmail.com
Navya M: 0009-0001-7770-0158
Sandeep S: 0000-0003-3466-7324
Anil Kumar: 0009-0001-6766-6339
DOI: https://doi.org/10.56093/CR.v42i1.3

lepidolite (potassium–lithium) and zinnwaldite (lithium–iron) (Lauf., 2006).

The commonly occurring natural micas are phlogopite, biotite, and muscovite. Among the natural micas, muscovite has a dioctahedral structure with potassium as the interlayer cation and studies have showed that it is difficult to dissolve and exchange the potassium in the muscovite interlayers with other cations (Kalinowski and Schweda, 1996). Unlike muscovite, the biotite ($K(Mg,Fe)_3AlSi_3O_{10}(OH)_2$) has a trioctahedral structure, rich in magnesium and iron and exhibits a high cation exchange capacity. Phlogopite, is a magnesium-bearing mica. Phlogopite deposits are mainly associated with metamorphosed limestone and mafic rocks and occur particularly in hydrothermal veins formed through metasomatism of magnesium rich rocks, such as dolomite (Harben and Ku•vart 1996).

Recently, the handling of waste mica has garnered significant interest due to its large production volume. Besides mining of mica, quarrying of coarse materials like granite (Hojamberdiev *et al.,* 2011), phyllosilicates like china clay (Zografou *et al.,* 2014) and valuable materials like gold, copper, uranium, and platinum (Nosrati *et al.,* 2009; Basak, 2019) are the important sources of waste mica. During the dressing of raw mica, approximately 75% of the material is discarded as waste close to the mica mines, which primarily consist of muscovite (white mica) and biotite (black mica) (Villaros and Pichavant, 2019). These wastes are generally homogeneous, fine, and loose, with low moisture-holding capacity, low bulk density, and lack nutrients. They can also contaminate the environment during monsoons and strong winds (Kumar and Maiti, 2015; Monnier *et al.,* 2022). However, low grade potassium bearing minerals, such as feldspar and waste mica are gaining importance as a means to reduce reliance on imported or commercial potassium fertilizers due to its significant potassium content (Badr *et al.,* 2006; Nishanth and Biswas, 2008; Basak and Biswas, 2009; Basak and Biswas, 2010). In the Scandinavian countries, crushed rocks rich in K-feldspar (Bowie *et al.,* 1966) have been used as a long-term K-fertilizer in organic farming.

In the present study, waste mica was collected from mica mines, and subjected to various characterization techniques to determine the type and its potential as a potassium source.

Materials and Methods

Materials

The waste mica was collected from mica mining sites in Andhra Pradesh and used in the study. Prior to different characterizations, they were gently crushed and finely ground to a particle size that passed through a 0.2 mm sieve.

Characterization of waste mica: Characterizations of the waste mica were done by using X-ray fluorescence spectrometer (XRF), X-ray diffraction (XRD), fourier transformed infrared spectroscopy (FTIR), and scanning electron microscopy (SEM).

Chemical composition and elemental formula: Important elemental oxides present in waste mica were determined by a SPECTRO XEPOS spectrometer with an X-ray tube with a thick binary Pd/Co alloy anode with air-cooling operated at 50 Kv and 50 W. After determining the elemental composition, the chemical formula of the waste mica was calculated from its chemical composition in terms of the percentage of oxide of its constituent elements (Datta, 2022). Briefly,

1. Each oxide was divided by its molecular weight and then multiplied by the number of cations present in the oxide to calculate the moles of cation per 100 grams of the sample.
2. The moles of each cation were converted to equivalents of cations per 100 grams of the sample by multiplying the moles with the valency of the cation.

3. The equivalents of all cations were summed to obtain S. The ratio R of 44 to S were calculated, where 44 is the total number of equivalents or charge of cations present in unit cell or formula of 2:1 mineral. Finally, the moles of each cation were multiplied by R to determine the actual number of atoms per formula weight.
4. Deriving the formula:
   a) The moles of K and X were assigned to the interlayer position as exchangeable cation.
   b) The moles of Si were assigned to tetrahedral position and a portion of Al is also assigned to tetrahedral position to make total moles on tetrahedral sheet as 8.
   c) The rest amount of Al is assigned to octahedral position. Besides Al, the other elements such as Mg and Fe were assigned to octahedral sheet as per their mole number.
   d) The moles of oxygen and OH were assumed to be equal to 20 and 4, respectively.

X-ray diffraction (XRD): XRD patterns of waste mica were obtained using an X-ray diffractometer (Rigaku Corporation, Japan, Model: Miniflex 6G) with Cu Kα radiation (λ = 0.154 nm) at 40 kV and 15 mA. For the identification of minerals in the mine spoils, samples were saturated with calcium and solvated with ethylene glycol. A subset of samples was also saturated with potassium at 25°C and heated to 110°C, 300°C, and 550°C. After Ca and K saturation, waste mica was characterized using XRD. The patterns of XRD were recorded in the range of 3–60° with a scanning speed of 2° min^{-1} and a step width of 0.01°.

Fourier transformed infrared spectroscopy (FTIR): Attenuated Total Reflectance (ATR) mode was used for Fourier Transform Infrared Spectroscopy (FTIR) characterization (Perkin Elmer Inc., USA, Model: SPECTRUM TWO). The measurement of spectra was in the range of 4000–450 cm^{-1} with 16 scans at a resolution of 4 cm^{-1} at room temperature.

Scanning electron micrographs (SEM): The morphological features of the waste mica were captured by scanning electron microscopy (Jeol 6390LA/OXFORD XMX N) at an accelerating voltage of 0.5 to 30 kV.

Bioavailability Experiments

The potassium bioavailability experiment was conducted for analysing the potential of waste mica as a nutrient source. The bioavailability experiments were carried out based on the methodologies reported by Adhikari *et al.,* 2015 and Dutta *et al.,* 2019, with minor modifications to suit the objectives of this study. *Triticum aestivum* (variety: Gw 322) seeds were used to assess the potential of waste mica as a K source. To determine the seed germination rate, seeds were germinated in petri plates with dimensions of 100 × 15 mm^2 for about 3 days after sterilization and water soaking. The dimension of the petri plates was adequate to support the plant growth for the duration of our experiments (8 days) (Lin *et al.,* 2009). The average germination rates of seeds were greater than 90%. Three treaments vis – a – vis T1 = control; T2 = nutrient solution only and T3 = half of the recommended dose of potassium as waste mica (40 kg ha^{-1}) along with nutrient solution was used in this study. Three replicates were maintained for each treatment. The nutrient solution was a modified hoagland solution prepared using ammonium dihydrogen phosphate ($NH_4H_2PO_4$), potassium nitrate (KNO_3), calcium nitrate ($Ca(NO_3)_2$, magnesium sulphate ($MgSO_4$), boric acid (H_3BO_3), manganese chloride ($MnCl_2$), copper sulphate ($CuSO_4$), zinc sulphate and molybdic acid ($MoO_3 . H_2O$) (Table 1).

The growth medium was quartz sand which was washed several times and placed in a

Table 1. Composition of the Nutrient Solution (Half Strength Modified Hoagland Solution)

Nutrient	ml L^{-1} of nutrient solution
1 M $NH_4H_2PO_4$	0.50
1 M KNO_3	3.00
1 M Ca $(NO_3)_2$	2.00
1 M $MgSO_4$	1.00
100 ppm B (H_3BO_3)	2.50
100 ppm Mn ($MnCl_2$)	2.50
10 ppm of Cu ($CuSO_4$)	1.00
10 ppm $ZnSO_4$	1.00
10 ppm Mo (molybdic acid)	0.50

microwave oven for 10 minutes. 10 g of quartz sand was used in each petri plate to grow the seedlings. For T3, the quartz sand (10 g) was mixed with waste mica at a dose as mentioned above. Four germinated seeds/ seedlings were planted in each plate and it was ensured that the roots of the seedlings were kept submerged in sand throughout the experiment. The seedlings were allowed to grow for 8 days, and nutrient solution (half strength modified Hoagland solution) was added (6 to 8 mL per day) starting from the second day of the experiment. The plants were grown under controlled environmental conditions with a day/night temperature regime of 25°C/18°C; 12h/12h light/dark cycle for 8 days.

At the end of the experiment, the plants were harvested, and the root samples were gently washed with tap water and then with deionised water to get rid of sand particles. The root length was measured. For the measurement of K, roots and shoots were separated from seedlings and the fresh weight of roots and shoots measured. The samples were dried in an oven at 70°C till constant weights were recorded. Thereafter, the dried plant samples were ground, and the powdered samples were acid digested. Potassium (K) content in the digests was determined by inductively coupled plasma (ICP) (Model: PERKIN ELMER AVIO 200).

Results and Discussions

Elemental Composition

The XRF analysis was performed to determine the elemental composition of the waste mica and presented in Table 2. The elemental formula of the waste mica was calculated based on the elemental composition results. The XRF analysis shows that 49.23% of the constituent elemental oxides in the waste mica was comprised of SiO_2, while 18.26% was constituted by Al_2O_3, 15.45% by MgO, and 11.28% by Fe_2O_3. Additionally, the sample exhibited the presence of 3.81% K_2O. Based on the composition, the elemental formula of waste mica was computed as $(X_{0.34}K_{0.61})$ interlayer $(Si_{6.13}Al_{1.87})^{IV}(Al_{0.86}Mg_{2.88}Fe_{1.06}Ti_{0.15})^{VI}O_{20}(OH)_4$ (Table 3). The elemental composition analysis indicates a high percentage of iron and magnesium, indicating biotite as the dominant micaceous mineral in these mine spoils (Haldar, 2020). Studies by Abdel Rahman (1994) on the composition of biotite from various igneous rock types concluded that biotites in alkaline anorogenic suites are mostly iron-rich, while those in peraluminous (including S-type) suites are siderophyllitic in composition, and the ones in calc-alkaline (mostly subduction-related orogenic suites) are enriched in Mg.

The Mg/Fe ratio of the studied samples were 1.18, further confirming that the waste mica/

Table 2. Elemental composition, Si/Al ratio, and Mg/ Fe ratio of waste mica

Elemental Oxides	Composition (in mass %)
SiO_2	49.23
Al_2O_3	18.26
MgO	15.45
Fe_2O_3	11.28
K_2O	3.81
Si/Al ratio	2.38
Mg/Fe ratio	1.18

Table 3. Calculation of elemental formula of the mica mineral in mine spoils

Cation Oxide	Oxides (%)	Molecular Weight	Moles Cation/100 g	Equivalent of cation/100 g (Moles*Valency)	R=44/5.894	No of atoms per unit cell or formula weight (moles/100g*R)
SiO_2	49.23	60	0.821	3.282	7.47	6.13
Al_2O_3	18.26	100	0.365	1.096		2.73
MgO	15.45	40	0.386	0.773		2.88
Fe_2O_3	11.28	159.6	0.141	0.424		1.06
K_2O	3.81	94	0.081	0.195		0.61
TiO_2	0.74	75	0.020	0.079		0.15
X (exch. cation)			0.023	0.046		0.34
Sum				5.894		
Elemental Formula	$(X_{0.34}K_{0.61})^{INTERLAYER}(Si_{6.13}Al_{1.87})^{IV}(Al_{0.86}Mg_{2.88}Fe_{1.06}Ti_{0.15})^{VI}O_{20}(OH)_4$					

micaceous mineral could be indeed biotite. According to Deer *et al.* (1992), phlogopites exhibit a Mg/Fe ratio greater than 2, while biotite features a Mg/Fe ratio less than 2. Further, the Fe/(Fe+Mg) ratio was found to be 0.46 indicating that the dominant mineral was positioned near the siderophyllite-eastonite boundary of the International Mineralogical Association (IMA) classification diagram, a common position for biotite micas (Rieder *et al.,* 1998).

XRD Analysis

XRD spectra of the waste mica showed characteristic well-defined diffraction peaks of mica at 2θ angles of 8.99° and 26.81° (*d* values = 0.98 nm and 0.33 nm, respectively) (Fig 1a).

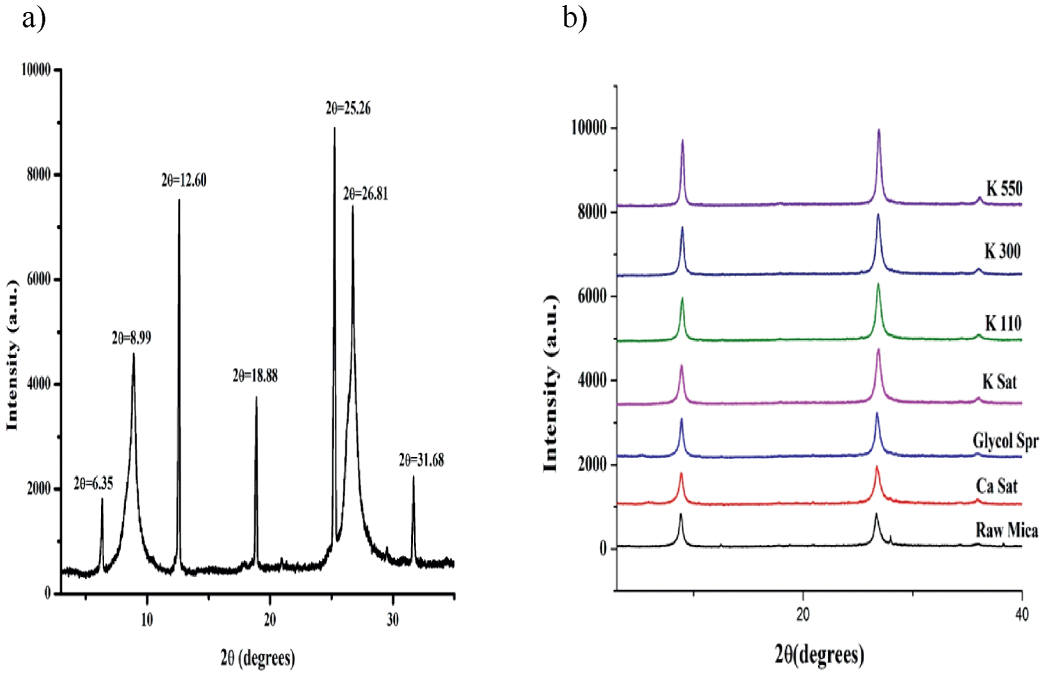

Fig. 1 a - b: XRD results of a. random oriented sample and b. Ca - EG and K saturation results of waste mica

White (1962) suggested that, as the dioctahedral micas (muscovite) are depleted of their K, the intensity of the (001) reflection should increase more quickly than that of the (002) reflection and a reverse effect could hold true for trioctahedral micas. The values of the intensity ratio (001)/(002) (peak height) of waste mica in the present study was found to lie between 1 and 3, hence confirming that the waste mica obtained from the mines is trioctahedral biotite and is in good agreement with those reported by White (1962).

FTIR Analysis

The samples exhibited characteristic well-defined bands of mica at 987 cm^{-1} and 731 cm^{-1} associated with its tetrahedral and octahedral structural components, intercalated water, and hydroxyl groups (Fig. 2). Generally, the ν(Si–O–Si) modes are responsible for bands that are seen in 1100–900 cm^{-1} spectral region, whereas the stretching modes of octahedral Al–O and Al– O–Al would lead to specific bands at 900–740 cm^{-1} (Šontevska *et al.,* 2008). The most intense maximum in the spectra of the samples was observed around 987 cm^{-1} attributed to the ν(Si–O–Si) vibrations and being in good agreement with the earlier FTIR studies for biotite mica (Zeller, 1975; Šontevska *et al.,* 2008).

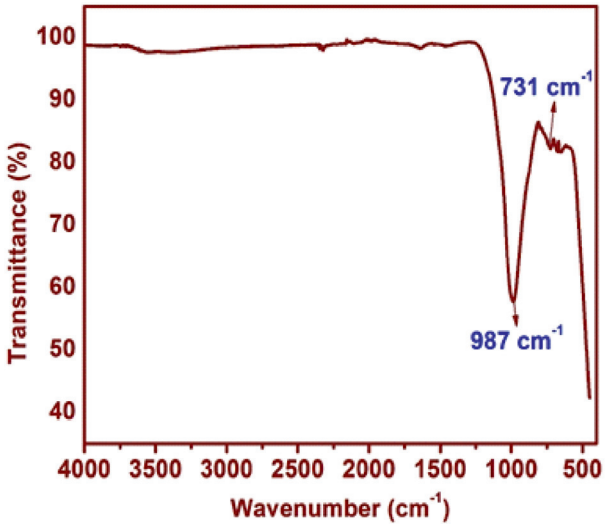

Fig. 2. FTIR spectra of waste mica

Scanning Electron Microscopy

The SEM images of the waste mica are presented in Fig. 3. The images show that the samples were crystallined in a monoclinic form with tabular/prismatic crystals in a pinacoid termination. Further, the morphological features depicted two pinacoid faces and four prism faces forming a pseudo-hexagonal structure of biotite. Muscovite, on the other hand, would have shown crystallized structures in a monoclinic system, forming amorphous pseudo-crystals (Rickwood, 1981; Hosseini, 2000).

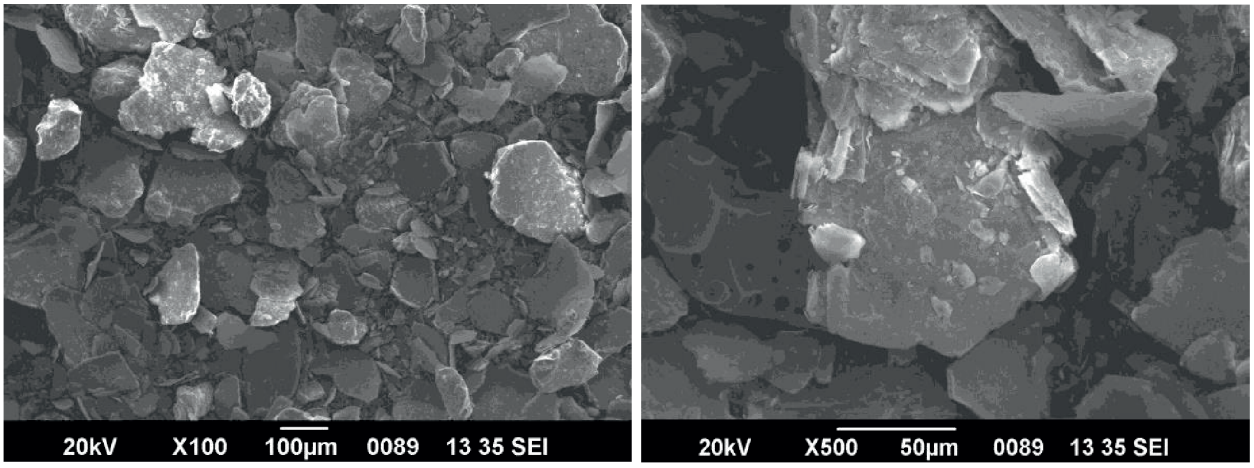

Fig. 3. SEM Images of waste mica

Bioavailability Experiments

The effects of waste mica on the growth of wheat plants (*Triticum aestivum*) were investigated for 8 days period. The results show that wheat plants responded well to the application of waste mica along with nutrient solution, as it resulted in better growth than nutrient solution only and control treatments, (Figure 4, Table 4). Plants treated with a combination of waste mica and nutrient solution exhibited greater height (17.17±1.70 cm) compared to those receiving only the nutrient solution (16.55±1.09 cm). The wheat plants applied with half of the recommended potassium through waste mica along with nutrient solution had a comparable effect on shoot height, shoot dry weight, root length, and the shoot and root potassium content with respect to wheat plants applied with nutrient solution only. Results of the ICP analysis (Table 5) of plant digests show greater concentration of potassium in the shoot and roots of wheat plants treated with waste mica along with nutrient solution than the nutrient solution only. Waste mica, a potassium-rich orthoclase-type aluminosilicate mineral (Brady, 2003), serves as a source of potassium. In mica, potassium atoms are located in interlayer positions between two expandable aluminosilicate sheets and are released gradually, supporting sustained plant growth under controlled conditions (Xiao *et al.,* 2017). This study indicated that waste mica could be considered

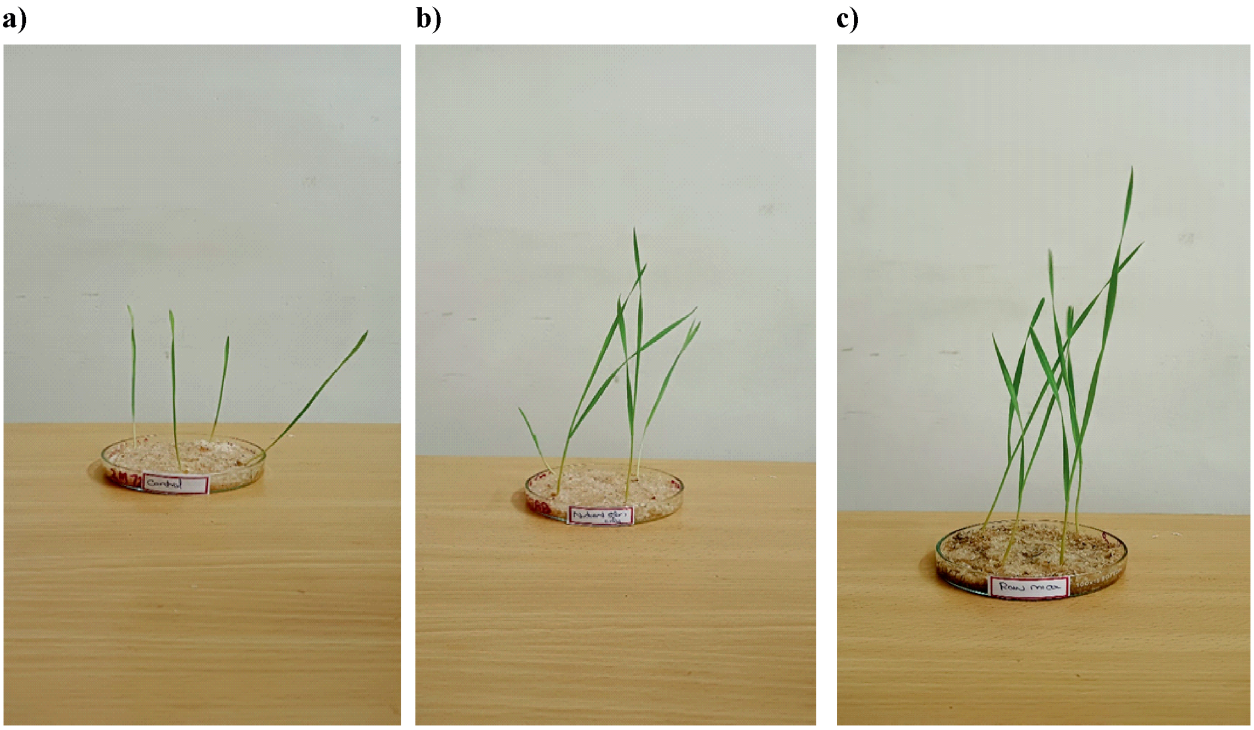

Fig. 4. Growth of wheat (*Triticum aestivum*) plant under (a) control, (b) nutrient solution only, (c) waste mica

Table 4. Growth parameters of wheat plants after 8 days of incubation with waste mica

Treatment	Shoot Height	Shoot Dry Weight	Root Length	Root Dry Weight
Control	10.92±0.46	0.04±0.002	8.35±0.04	0.03±0.003
Nutrient Solution only	16.55±1.09	0.05±0.003	13.00±0.90	0.05±0.001
Waste Mica	17.17±1.70	0.06±0.006	13.45±1.24	0.05±0.005

Table 5. Shoot and root nutrient content of wheat plants after 8 days of incubation with waste mica

Treatment	Shoot K content (mg/L)	Root K content (mg/L)
Control	4565±1.73	1820.5±1.15
Nutrient Solution only	14672.5±1.65	4892.5±1.46
Waste mica	16602.5±1.96	6195±0.96

an effective potassium/nutrient source for plant growth. Field experiments are necessary to optimize the combination of waste mica and nutrients and this could be a viable low-cost potassium management strategy that could auger well with the concept of waste to wealth strategy.

Conclusion

This study successfully identified the collected waste mica as biotite, with elemental analysis, particularly the high iron content, playing a pivotal role in its classification. The Mg/Fe ratio and structural features supported by XRD, FTIR and SEM results validated this identification. The bioavailability experiments showed that the waste mica/biotite significantly enhances nutrient availability, leading to better plant growth compared to other treatments. These findings underscore the potential of waste mica as effective sustainable plant nutrient source. Future studies should focus on long-term effects and scalability in agricultural applications.

Acknowledgements

The authors acknowledge the support from the Kerala State Council for Science, Technology and Environment (KSCSTE), KSCSTE- Kerala Forest Research Institute, Cochin University of Science and Technology (CUSAT), STIC CUSAT, and CSIF-University of Calicut.

Conflict of Interest

There are no conflicts of interest to declare.

Contribution of authors

Navya M: Data curation, formal data analysis and writing of the original manuscript

Dr. Sandeep S: Supervision, review and editing of the manuscript

Dr. Anil Kumar: Editing and fine tuning of the manuscript

References

Abdel-Rahman A.F.M. 1994. Nature of biotites from alkaline, calc-alkaline, and peraluminous magmas. Journal of Petrology. **35**: 525–541.

Adhikari T., Kundu S., Biswas A.K., Tarafdar J.C. and Subba Rao A. 2015. Characterization of zinc oxide nanoparticles and their effect on growth of maize (Zea mays L.) plant. Journal of Plant Nutrition. **38**(10): 1505–1515.

Andric L., Terzic A., Pavlovic L. and Petrov M. 2014. Comparative kinetic study of mechanical activation process of mica and talc for industrial application. Composites Part B: Engineering. **59**: 181–190.

Badr M.A., Shafei A.M. and Sharaf El-Deen S.H. 2006. The dissolution of K and P-bearing minerals by silicate dissolving bacteria and their effect on sorghum growth. Research Journal of Agriculture and Biological Sciences. **2**: 5–11.

Basak B.B. 2019. Waste Mica as Alternative Source of Plant-Available Potassium: Evaluation of Agronomic Potential Through

Chemical and Biological Methods. Natural Resources Research. **28**(3): 953–965.

Basak B.B. and Biswas D.R. 2009. Influence of potassium solubilising microorganism (Bacillus mucilaginosus) and waste mica on potassium uptake dynamics by sudan grass (*Sorghum vulgare Pers.*) grown under two Alfisols. Plant and Soil. **317**: 235-255.

Basak B.B. and Biswas D.R. 2010. Co-inoculation of potassium solubilizing and nitrogen fixing bacteria on solubilization of waste mica and their effect on growth promotion and nutrient acquisition by a forage crop. Biology and Fertility of Soils. **46**: 641-648.

Bowie S. H. U., Dawson J., Gallagher M. J. and Ostle D. 1966. Potassium-rich sediments in the Cambrian of Northwest Scotland. Transactions of the Institution of Mining and Metallurgy. **75**: 125-142.

Brady N. 2003. The nature and properties of soil, Colier McMillan, London, 960 pp.

Datta S. C. 2022. Characterization of Soil Minerals-I. In Text book on Physical Chemistry and Mineralogy of Soils, Directorate of Knowledge Management in Agriculture, Indian Council of Agricultural Research, Pusa, New Delhi.

Deer W.A., Howie, R.A. and Zussman, J. 1992. An Introduction to the Rock-Forming Minerals, Longman Scientific & Technical, London, 696 pp.

Dutta T., Bagchi D., Bera A., Das S., Adhikari T. and Pal S.K. 2019. Surface engineered ZnO-humic/citrate interfaces: Photoinduced charge carrier dynamics and potential application for smart and sustained delivery of Zn micronutrient. ACS Sustainable Chemistry & Engineering. **7**(12): 10920–10930.

Fanning D.S. and Keramidas V.Z. 1977. Micas. In (J.B. Dixon and S.B. Weed Ed.) Minerals in soil environments, Soil Science Society of America, Madison, pp. 195–258.

Haldar S. K. 2020. Introduction to mineralogy and petrology, Elsevier, Amsterdam, Netherlands, 419 pp.

Harben P.W. and Ku•vart M. 1996. Industrial minerals: a global geology, Industrial Minerals Information Ltd, London, 462 pp.

Hojamberdiev M., Eminov A. and Xu Y. 2011. Utilization of muscovite granite waste in the manufacture of ceramic tiles. Ceramics International. **37**(3): 871–876.

Hosseini E. 2000. Crystals and Minerals, Ruykard-e Novin Publishing Cooperation, Tehran, Iran.

Kalinowski B. E. and Schweda P. 1996. Kinetics of muscovite, phlogopite, and biotite dissolution and alteration at pH 1–4, room temperature. Geochimica et cosmochimica acta. **60**(3): 367-385.

Kumar A. and Maiti S. K. 2015. Assessment of potentially toxic heavy metal contamination in agricultural fields, sediment, and water from an abandoned chromite-asbestos mine waste of Roro hill, Chaibasa, India. Environmental Earth Sciences. **74**: 2617-2633.

Lauf R. J. 2006. Collector's Guide to the Mica Group. Rocks & Minerals. **81**(3): 214-224.

Lin S., Reppert J., Hu Q., Hudson J. S., Reid M. L., Ratnikova T. A., Rao A. M., Luo, H. and Ke P. C. 2009. Uptake, translocation, and transmission of carbon nanomaterials in rice plants. Small. **5**(10): 1128–1132.

Monnier L., Salvi S., Melleton J., Lach P., Pochon A., Bailly, L. and De Parseval P. 2022. Mica trace-element signatures: Highlighting superimposed W-Sn mineralizations and fluid sources. Chemical Geology. **600**: 120866.

Nishanth D. and Biswas D. R. 2008. Kinetics of phosphorus and potassium release from rock phosphate and waste mica enriched compost and their effect on yield and nutrient uptake by wheat (*Triticum aestivum*). Bioresource

technology. **99**: 3342–3353.

Nosrati A., Addai-Mensah J. and Skinner W. 2009. pH-mediated interfacial chemistry and particle interactions in aqueous muscovite dispersions. Chemical engineering journal. **152**(2–3): 406–414.

Pérez-Rodríguez J. L., Wiewióra A., Drapala J. and Pérez-Maqueda L. A. 2006. The effect of sonication on dioctahedral and trioctahedral micas. Ultrasonics sonochemistry. **13**(1): 61-67.

Rickwood P. C. 1981. The largest crystals. American Mineralogist. **66**(9-10): 885-907.

Rieder M., Cavazzini G., D'Yakonov Y.S., Frank-Kamenetskii V.A., Gottardi G., Guoggenheim S., Koval P.V., Muller G., Neiva A.M.R., Radoslovich E.W., Robert J,L., Sssi F.P., Takeda H., Weiss Z. and Wones D.R. 1998. Nomenclature of the micas. Clays and Clay Minerals. **36**: 41–48.

Šontevska V., Jovanovski G., Makreski P., Raškovska A. and Šoptrajanov B. 2008. Minerals from Macedonia. XXI. Vibrational spectroscopy as identificational tool for some phyllosilicate minerals. Acta Chimica Slovenica. **55**(4): 757–766.

Villaros A. and Pichavant M. 2019. Mica-liquid trace elements partitioning and the granite-pegmatite connection: The St-Sylvestre complex (Western French Massif Central). Chemical Geology. **528**: 119265.

White J. L. 1962. X-ray diffraction studies on weathering of muscovite. Soil Science. **93**(1): 16-21.

Xiao Y., Wang X., Chen W. and Huang Q. 2017. Isolation and identification of three potassium-solubilizing bacteria from rape rhizospheric soil and their effects on ryegrass. Geomicrobiology Journal. **34**: 873–880.

Zeller M. V. 1975. Infrarot-Vergleichsspektren von Mineralien, Bodenseewerk, Perkin-Elmer.

Zografou A. Heath A. and Walker P. 2014. China clay waste as aggregate in alkali- activated cement mortars. Proceedings of the Institution of Civil Engineers-Construction Materials. **167**(6): 312–322.

(Received: 15 December 2024; Accepted: 31 January 2025)